Supporting Information

Dextransucrase-Catalyzed Elongation of Polysaccharide Brushes with Immobilized Mono-/Di-saccharides as Acceptors

Yan Fang[a], Jian Wu[b] and Zhi-Kang Xu*[a]

[a]MOE Key Laboratory of Macromolecular Synthesis and Functionalization, Department of Polymer Science and Engineering, Zhejiang University, Hangzhou 310027, China

[b]Department of Chemistry, Zhejiang University, Hangzhou 310027, China

Materials and methods

Materials. Sigma-Aldrich (China) provided the following commercial products and they were used as received: 11-mercapto-1-undecanol (MUD), dextransucrase (DSase) from *Leuconostoc mesenteroides*, concanavalin A (Con A), fluorescent isothiocyanate-labeled concanavalin A (FITC-Con A), *ricinus communis agglutinin* (RCA_{120}), fluorescent isothiocyanate-labeled *ricinus communis agglutinin* (FITC-RCA_{120}) and bovine serum albumin (BSA). Fluorescent isothiocyanate-labeled bovine serum albumin (FITC-BSA) was a product from Shanghai Jing-Tian Biotech. Inc. (China). β-D-glucose Pentaacetate (GPA, 99%), β-D-maltose Octaacetate (MOA, 99%), and methyl α-D-mannopyranoside (MM) (99%) were purchased from *J&K* Chemical (China). Boron trifluoride diethyl etherate ($BF_3 \cdot Et_2O$) was a commercial product from Shanghai ling-feng chemical reagent Inc. (China). Sucrose, ethanol, acetic acid, sodium chloride (NaCl), calcium chloride ($CaCl_2$), manganese chloride ($MnCl_2$), sodium methoxide, dichloromethane and all the other chemicals were purchased from Sinopharm (China) and used as received without further purification. A 50.0 mM acetic acid-sodium acetate buffer solution (pH 5.2) containing 0.15 M NaCl and 1 mM $CaCl_2$ was used as the buffer solution for the enzymatic polymerization reaction. Phosphate-buffered saline solution (PBS, 0.1 M, pH 7.3) containing 0.1 mM $CaCl_2$, 0.1 mM $MnCl_2$, and 0.1 M NaCl solution was used for affinity dissociating Con A. PBS (0.1 M, pH 7.3) containing 0.1 mM $CaCl_2$ and 0.1 M NaCl was used for dissociating RCA_{120} and BSA. Water used in all experiments was deionized and ultra-filtrated to 18 MΩ·cm using an ELGA Lab Water system (France).

The commercially available QCM gold sensor chip was comprised of a bare gold surface (Q-sense SX-301, Q-SENSE, Sweden). The chip was rinsed with ethanol and dried under a gentle stream of ultra-pure N_2 gas, after which it was placed in a 1:1:5 mixtures of ammonia (28%), hydrogen peroxide (30%), and ultra-pure water, at ~60 ^oC for 10 min. Subsequently, the chip was thoroughly rinsed with ultra-pure water and ethanol, and then dried under a steady stream of ultra-pure N_2 gas for further use.

Preparation of saccharide acceptors immobilized surfaces. As the acceptor substrate for DSase, glucose and maltose were immobilized on QCM via a typical procedure. Firstly, 5.0 mM MUD was dissolved in ethanol and oxygen was removed from the solution by nitrogen bubbling for 5 min. Then, the chip was immersed in MUD solution for 12 h to form a self-assembly monolayer (SAM) on the chip surface. The surface was then rinsed in ethanol, dried under a gentle stream of ultra-pure N_2 gas, and immediately assembled into the QCM chamber for further use. GPA and MOA were subsequently immobilized onto the chip surface by covalent attachment to the Hydroxyl groups of MUD SAM. Briefly, GPA and MOA were dissolved in dry dichloromethane and oxygen was removed from the solution by nitrogen bubbling for 10 min. The SAM-modified chip was immediately immersed into the above solution and $BF_3 \cdot Et_2O$ was added as the catalyst for 24 h at ambient temperature. The surface was then rinsed in dichloromethane, ethanol, and dried under a gentle stream of ultra-pure N_2 gas. The obtained GPA and MOA modified chips were then immersed into sodium methoxide-ethanol solution (5 mg/mL) for 90 min at ambient temperature. Finally, the glucose and maltose immobilized chips were obtained (Scheme S1) and rinsed in ethanol and ultra-pure water, and then dried under a steady stream of ultra-pure N_2 gas for further use.

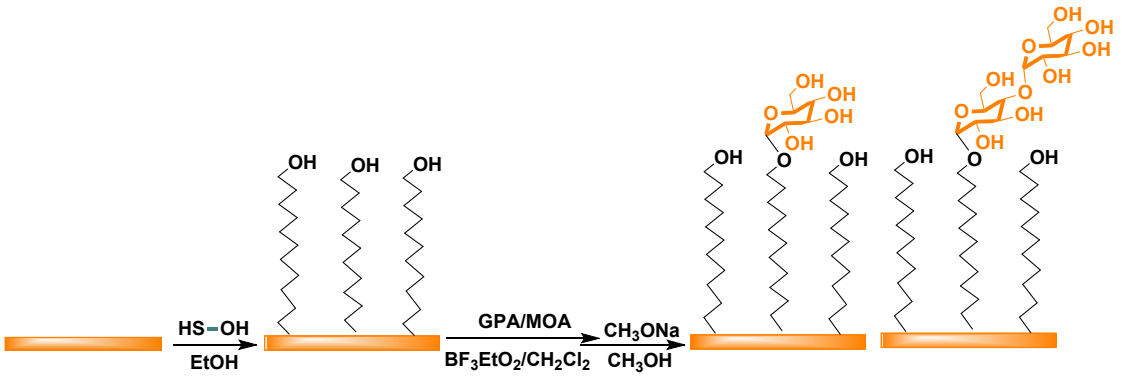

Scheme S1. Construction of glucose/maltose-terminated SAM surfaces.

DSase catalyzed elongation on the saccharide acceptors immobilized surface. The saccharide acceptors immobilized substrates were immerged in a 50.0 mM acetic acid-

sodium acetate buffer solution (pH 5.2) containing DSase (a certain concentration). The immersed substrates were incubated for 2 hours at 25 ^{o}C in a shaking incubator. Afterward, the substrates were thoroughly rinsed with ultra-pure water, and then immediately immerged in another 50.0 mM acetic acid-sodium acetate buffer solution (pH 5.2) containing sucrose (certain concentrations). The immerged substrates were incubated for a certain time at 37 ^{o}C in a shaking incubator. Afterward, the substrates were thoroughly rinsed with ultra-pure water, dried with steady stream of ultra-pure N_2 gas, and stored in vacuo.

Characterization

Ellipsometry. The variable-angle spectroscopic ellipsometry (VASE) spectra were collected on an MD-2000I spectroscopic ellipsometer (J.A. Woollam, USA) at an incident angle of 60°, 65°, 70° in a wavelength range of 500-1000 nm. A refractive index of 1.45 was assigned to the saccharide acceptors terminated SAM surfaces and the polysaccharide brushes. For data analysis, a two-layer model (Au and Cauchy) was used to calculate the thickness of the brushes. All measurements were conducted in dry air at room temperature. Three separate spots of each sample were measured to obtain a mean brush thickness and associated standard deviation.

Fig. S1 shows that the thickness of MUD SAM is 1.1 ± 0.2 nm. After the immobilization of glucose and maltose acceptors, the thicknesses increases to 1.34 ± 0.2 nm and 1.52 ± 0.2 nm, respectively, which are in good agreement with the molecular length of glucose and maltose. It is known the bond length of one glucose residue is 0.42 nm.[1] Taking 0.42 nm as unity, maltose would have a length of 0.42 × 2 = 0.84 nm. Since the glucose and maltose acceptors do not react with 100% of the hydroxyl group from MUD SAM, the thickness of the acceptor immobilized surface should have smaller thickness than the desired value. However, the thickness will be also affected by the aggregation and orientation states of the saccharide moieties immobilized on SAM. The above results should be strengthened by another assay (such as radiolabeling).

The average density profile (σ) of the immobilized glucose and maltose can now be calculated by equation (1).

$$\sigma = L\rho N_a/M_n$$

where L is the layer thickness obtained with ellipsometry (1.1 nm to the MUD SAM, 0.24 nm to the glucose and 0.42 to the maltose); ρ is the density of MUD (0.79 g mL^{-1}), glucose (1.58 g mL^{-1}) and maltose (1.76 g mL^{-1}); N_a is constant of Avogadro, and M_n is

the molecular weight of MUD (204 $gmol^{-1}$), glucose (180 $gmol^{-1}$), and maltose (342 $gmol^{-1}$), yielding a grafting density of 2.56 nm^{-2} for MUD SAM, 1.27 nm^{-2} for glucose, and 1.30 nm^{-2} for maltose. It means that only 50% of the hydroxyl group of MUD SAM reacted with the glucose and the maltose. This is consistent with the above guess. Furthermore, the thickness changes to 1.45 ± 0.2 nm and 2.45 ± 0.2 nm after enzymatic elongation. It indicates that DSase catalyzed elongation is successful on the saccharide acceptors immobilized SAM surfaces and the corresponding degree of elongation is higher for the maltose acceptor than the glucose one. Based on the layer thickness, the amount of the introduced glucose residues was calculated to be 1~2 for the glucose immobilized surface and 7~8 for the maltose immobilized surface. (Previous work has determined the pitch of the helical structure of amylase is 0.8 nm with 6 glucose residues per turn.[2])

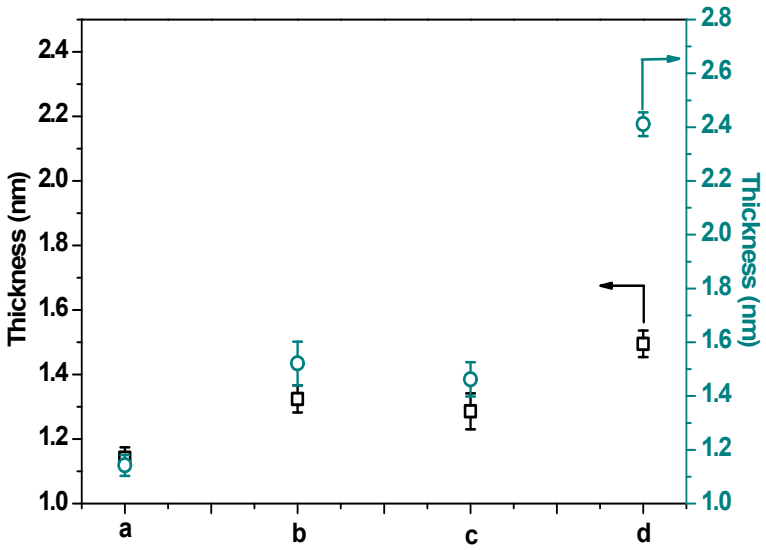

Fig. S1. Thickness changes of the surfaces measured by ellipsometry: a. MUD surface; b. the GPA- (□) and MOA- (○) immobilized surfaces; c. the glucose- (□) and maltose- (○) immobilized surface; d. the glucose- (□) and maltose- (○) immobilized surface after enzymatic polymerization.

Water contact angle (WCA). WCA was determined using a CTS-200 system (Mighty Technology Pvt. Ltd., China) fitted with a drop shape analyzer. Typical experiment was carried out at room temperature by sessile drop method as follows. Briefly, a water drop (2.0 μL) was lowered onto the chip surface from a needle tip. Then, the images of the droplet were recorded. WCAs were calculated from these images with software. At least five different surface locations of each sample were measured and the averaged value was presented.

Typical results are shown in Fig. S2. Compared to the bare gold surface (WCA is about 53° ± 2°), WCA of the SAM decreases to 40° ± 2° due to the hydroxyl group of MUD. After acetylated glycosides were introduced on the surfaces the WCA increases to 53° ± 2° for the GPA immobilized surface and 55° ± 2° for the MOA immobilized one. This may be attributed to the hydrophobicity of the acetylated glycosides molecules. After deacetylation, WCA is 36° ± 2° and 35° ± 2° for the glucose and the maltose immobilized surfaces, respectively. The hydrophilicity of the surface is expected from the numerous OH groups of the glucose and maltose unit. After enzymatic elongation, WCA continuously decreases to 32° ± 2° for the glucose immobilized surface and 30° ± 2° for the maltose immobilized surface. The high hydrophilic character of the surface is reasonable, not only due to the numerous OH groups but also the aliphatic carbon moieties of the formed polysaccharides.[3]

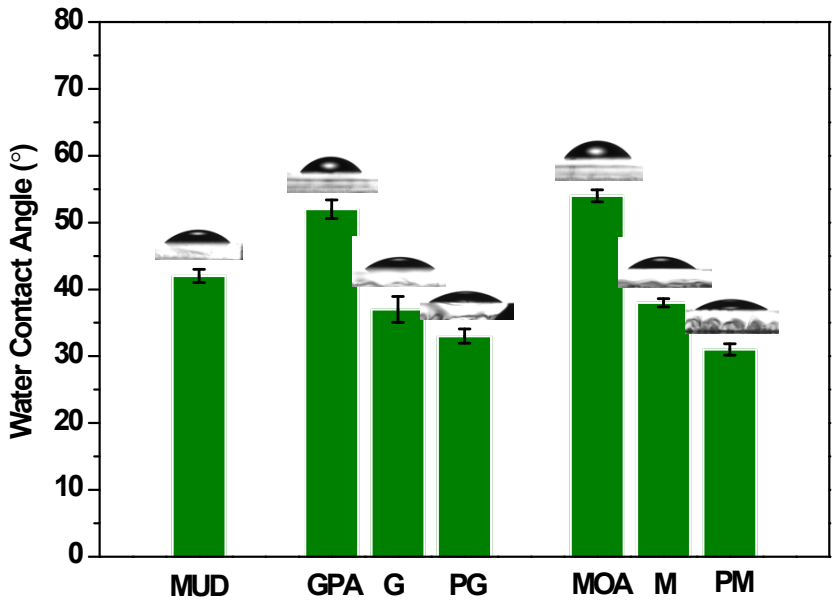

Fig. S2. Static WCA of different layers: That listed from left to right are MUD SAM (MUD); GPA terminated SAM surface (GPA); glucose acceptor terminated surface (G); glucose acceptor immobilized surface after enzymatic elongation (PG); MOA terminated SAM surface (MOA); maltose acceptor terminated surface (M); maltose acceptor immobilized surface after enzymatic elongation (PM).

QCM Monitoring. QCM analysis was carried out using a Q-SENSE E1 system (Q-SENSE, Sweden). The sensor crystals used were 5 MHz, AT-cut, polished quartz discs (chips) with electrodes deposited on both sides (Q-SENSE). The resonance frequency (*f*)

was measured simultaneously at four odd harmonics (5, 15, 25, 35 MHz). In the results, the values reported throughout for Δf was measured at the chosen fifth harmonics, unless otherwise stated. The working temperature was 25 °C. Raw data were analyzed with Origin Pro 8.0 (Origin-Lab, USA) and Q-Tools software (Q-SENSE).

DSase-catalyzed surface-initiated elongation. Enzymatic elongation experiments were conducted in real time using a Q-SENSE E1 system (Q-SENSE, Sweden). A peristaltic pump was used to deliver liquids to the channel of the flow cell. Figure S4 showed the above whole process. A stable baseline signal was established by flowing a 50.0 mM acetic acid/sodium acetate buffer solution (pH 5.2) containing 0.15 M NaCl and 1 mM $CaCl_2$ at a rate of 25 μL/min through the sensor. Then, DSase and sucrose solutions were injected into the channel, respectively. As can be seen from Fig. S3, a significant decrease occurs in QCM frequency upon interaction of the maltose acceptor with 80 nM injected enzyme. The frequency shows another decrease during the injection of sucrose (5 mM) for enzymatic elongation. After the enzymatic elongation for a fixed time at 25 °C, 1 M acetic acid solution was used to remove the affinity–bound enzyme from the newly prepared polysaccharide brushes. The enzymatic elongation is confirmed by the same decrease of frequency after thorough washing with the acetic acid solution. By contrast, the control surface (QCM chip) with MUD SAM, upon injecting the enzyme and the sucrose shows no change in frequency, although slightly similar decreases can be observed to the glucose acceptor immobilized surface (Fig. S4).

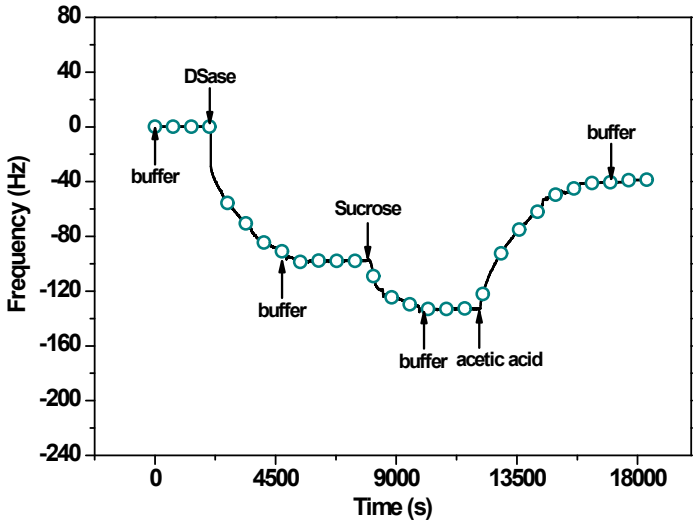

Fig. S3. Typical QCM curves (DSase-catalyzed surface-initiated polymerization) of the small saccharide acceptor immobilized surface. (Here, we choose the maltose acceptor

terminated SAM surface as the example.)

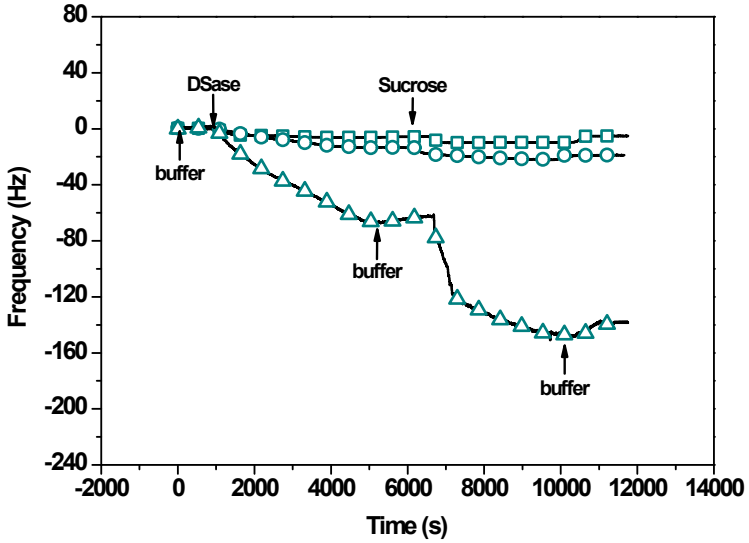

Fig. S4. Typical QCM curves (DSase-catalyzed surface-initiated elongation) of □: MUD SAM surface; ○: the glucose acceptor terminated SAM surface; Δ: the maltose acceptor terminated SAM surface.

Binding of DSase to the saccharide acceptors immobilized surfaces. QCM is a useful tool in the detection and quantitative analysis of each step in enzymatic reactions on the surface. In our cases, we can observe three steps continuously from time dependent frequency changes, which include 1) DSase binding to the small saccharide acceptors immobilized surfaces; 2) enzymatic elongation on the small saccharide acceptors immobilized surfaces, and 3) release of the enzyme from the newly constructed polysaccharide brushes. In the first step, DSase binding to the saccharide acceptor is described by Eq. S1. DSase/acceptor complex forms at time *t* after enzyme injection. The amount of the complex is given by Eq. S2 ~ S4.

$$acceptor + enzyme \underset{k_{off}}{\overset{k_{on}}{\rightleftharpoons}} acceptor/enzyme \quad \textbf{(S1)}$$

$$[acceptor/enzyme]_t = [acceptor/enzyme]_\infty \{1 - \exp(-t/\tau)\} \quad \textbf{(S2)}$$

$$\Delta m_t = \Delta m_\infty \{1 - \exp(-t/\tau)\} \quad \textbf{(S3)}$$

$$\tau^{-1} = k_{on}[enzyme] + K_{off} \quad \textbf{(S4)}$$

The relaxation time (τ) of DSase binding was calculated from curve fitting the QCM frequency changes at various DSase concentrations. DSase binding and dissociation rate constants (k_{on} and k_{off}) can be obtained from the slop and intercept of the plot of τ^{-1} against

DSase concentration. The dissociation constant (K_d) can also be obtained from the ratio of k_{off} to k_{on}. Fig. S5/S6 show the typical reciprocal plot of τ against DSase concentration to the glucose/ maltose acceptor immobilized surfaces. According to Eq. S4, the obtained k_{on} is 2.54 × 10^{-3} $M^{-1}S^{-1}$ and 3.99 × 10^{-3} $M^{-1}S^{-1}$ for the glucose and the maltose immobilized surfaces, respectively. k_{off} is 1.62 × 10^{-4} S^{-1} and 1.40× 10^{-4} S^{-1} for the glucose and the maltose immobilized surfaces, and K_d is 63.78 nM and 35.09 nM for the glucose and the maltose immobilized surfaces, respectively.

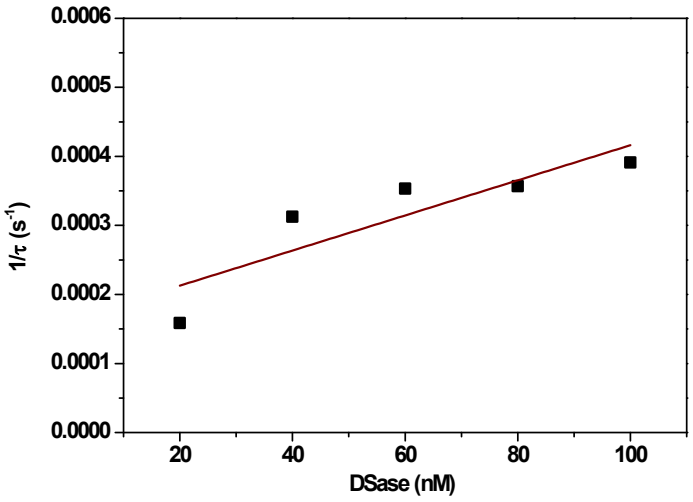

Fig. S5. Linear reciprocal plot of relaxation time τ against DSase concentration according to Eq. S4. (DSase binding on the glucose acceptor immobilized surface)

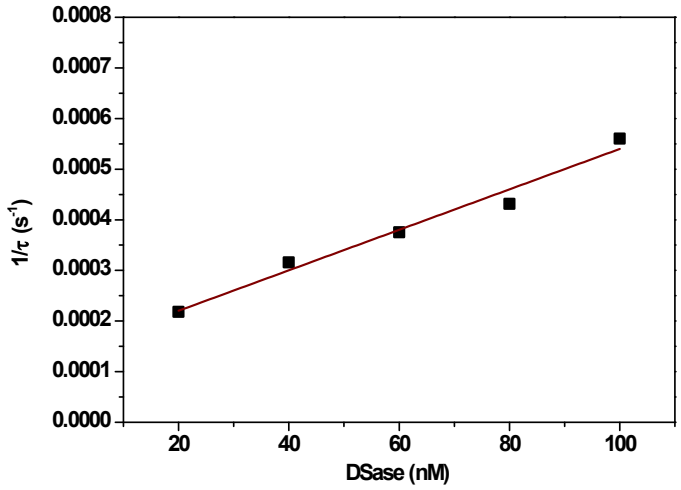

Fig. S6. Linear reciprocal plot of relaxation time τ against DSase concentration according to equation S4. (DSase binding on the maltose acceptor immobilized surface)

Enzymatic elongation starting from the immobilized saccharide acceptors. Enzymatic elongation occurs by adding sucrose after formation of DSase/acceptor complex on the QCM chip surface. The enzymatic elongation process is simply expressed by the *Michealis-Menten* model between the DSase/acceptor complex and the added sucrose as shown in Eq S5 ~ S7. The initial polymerization rate (v_0) increases with the addition of sucrose. From the reciprocal plot of v_0 against sucrose concentration, the Michaelis constant (K_m) and the catalytic polymerization constant (k_{cat}) were obtained from the slope and intercept of the plot.

$$acceptor / enzyme \underset{}{\overset{k_m}{\rightleftarrows}} acceptor / enzyme / sucrose \xrightarrow{k_{cat}} polysaccaride / enzyme$$

$$\textbf{(S5)}\quad v_0 = \frac{k_{cat}[acceptor / enzyme]_0[sucrose]}{k_m + [sucrose]_0}$$

(S6)

$$\frac{1}{v_0} = \frac{k_m}{k_{cat}[acceptor / enzyme]_0}\frac{1}{[sucrose]} + \frac{1}{k_{cat}[acceptor / enzyme]_0} \qquad \textbf{(S7)}$$

FT-IR/MR. FT-IR/MR measurements were performed using a Nicolet FT-IR (Thermo-Electron, Thermo Electron Corporation, USA) spectrometer equipped with an MR accessory. Thirty-two scans were taken for each spectrum at a resolution of 4 cm^{-1}.

FT-IR/MR can not detect any information of the MUD-SAM, the GPA/MOA immobilized surfaces and the glucose/maltose immobilized surfaces due to the relatively low content of the chemical composition on the surfaces and the lower resolution of the measurement. After enzymatic elongation, FT-IR/MR can detect some information on chemical composition and construction of the surfaces. Fig. S7 compares the FT-IR/MR spectra of the glucose/maltose acceptors immobilized surfaces after enzymatic elongation. It can be seen that the characteristic stretching vibration peak of the OH group of polysaccharides around 3500 cm^{-1}. Peaks around 1060 and 1250 cm^{-1}, which are typical absorptions of OH and CO groups, can be seen in the spectrum. The results preliminarily show that polysaccharides have been introduced to the surfaces by DSase-catalyzed surface-initiated elongation.

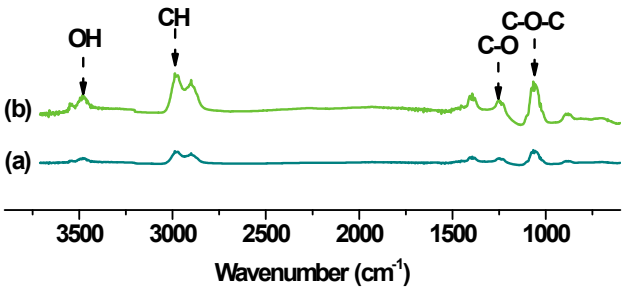

Fig. S7. FT-IR/MS spectra of surfaces after enzymatic elongation: (a) the glucose-immobilized surface; (b) the maltose-immobilized surface.

XPS analysis. XPS spectra were recorded on a PHI-5000C ESCA system (Perkin-Elmer, USA) with Al Kα excitation radiation (1486.6 eV). The pressure in the analysis chamber was maintained at 10^{-6} Pa during measurement. All spectra were referenced to the C_{1s} hydrocarbon peak at 284.6 eV to compensate for the surface charging effect. Table S1 summarizes the theoretical and experimental values of O/C for MUD-SAM (chemical formula $C_{11}OH_{23}S$), glucose terminated SAM (chemical formula $C_{17}O_6H_{34}S$) before and after enzymatic elongation, maltose terminated SAM (chemical formula $C_{23}O_{11}H_{44}S$) before and after enzymatic elongation. These data are in approximate agreement with the expected O/C values. As can be seen from Fig. S8, the slight decrease of O/C ratios seems plausible, as the O/C can be influenced by minor impurities at the surfaces, including carbon contamination of the gold surface due to environmental exposure after cleaning and other contaminants on the MUD, the saccharide acceptor immobilized surfaces or the polysaccharide brushes. Fig. S9 shows the high-resolution C1s XPS spectra for the MUD SAM surface, the saccharide acceptors immobilized surfaces, and the polysaccharide brushes surfaces. The C1s high-resolution spectrum of the MUD SAM surface (Fig. S9 (a)) shows that there is no significant acetal (O-C-O) peak at 288 ± 0.1 eV on the surface. And the C1s high-resolution spectrum for the glucose/maltose terminated SAM surfaces is fitted with three peaks: hydrocarbon (C-H/C-C/C-S) at 284.6 ± 0.1 eV, hydroxyl/ether (C-O-X) at 286.4 ± 0.1 eV, and acetal (O-C-O) at 288 ± 0.1 eV (Fig. S9 (b)/(c)). Compared with the saccharide acceptors immobilized surfaces, the C1s high-resolution spectrum of the polysaccharide brushes surface also can be fitted with three peaks: hydrocarbon (C-H/C-C/C-S) at 284.6 ± 0.1 eV, hydroxyl/ether (C-O-X) at 286.4 ± 0.1 eV, and acetal (O-C-O) at 288 ± 0.1 eV(Fig. S9 (d)/(e)). The O-C-O (288 ± 0.1) is unique to the saccharide acetal moiety. The proportion of O-C-O is increased significantly for the polysaccharide

brushes. Thus it can be included that DSase-catalyzed surface-initiated elongation has been carried out successfully. And there are more polysaccharides have been introduced to the maltose acceptor immobilized surface as compared with the glucose one.

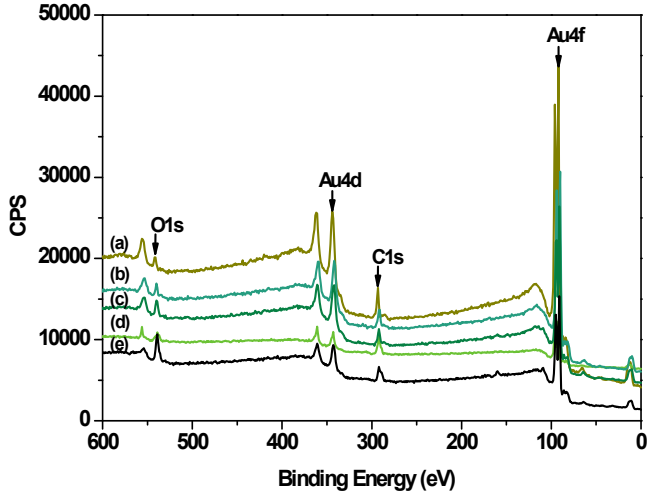

Figure S8. Survey XPS spectra: (a) MUD SAM surface, (b) the glucose-immobilized surface, (c) the glucose-immobilized surface after enzymatic polymerization, (d) the maltose-immobilized surface, (e) the maltose-immobilized surface after enzymatic polymerization.

Table S1. Theoretical and experimental values of O/C for each surface.

	surface[a]	surface[b]	surface[c]	surface[d]	surface[e]
theoretical O/C	0.091	0.35	0.83	0.48	0.83
experimental O/C	0.13	0.20	0.26	0.38	0.60

[a]MUD SAM surface, [b]the glucose-immobilized surface, [c]the glucose-immobilized surface after enzymatic polymerization, [d]the maltose-immobilized surface, [e]the maltose-immobilized surface after enzymatic polymerization.

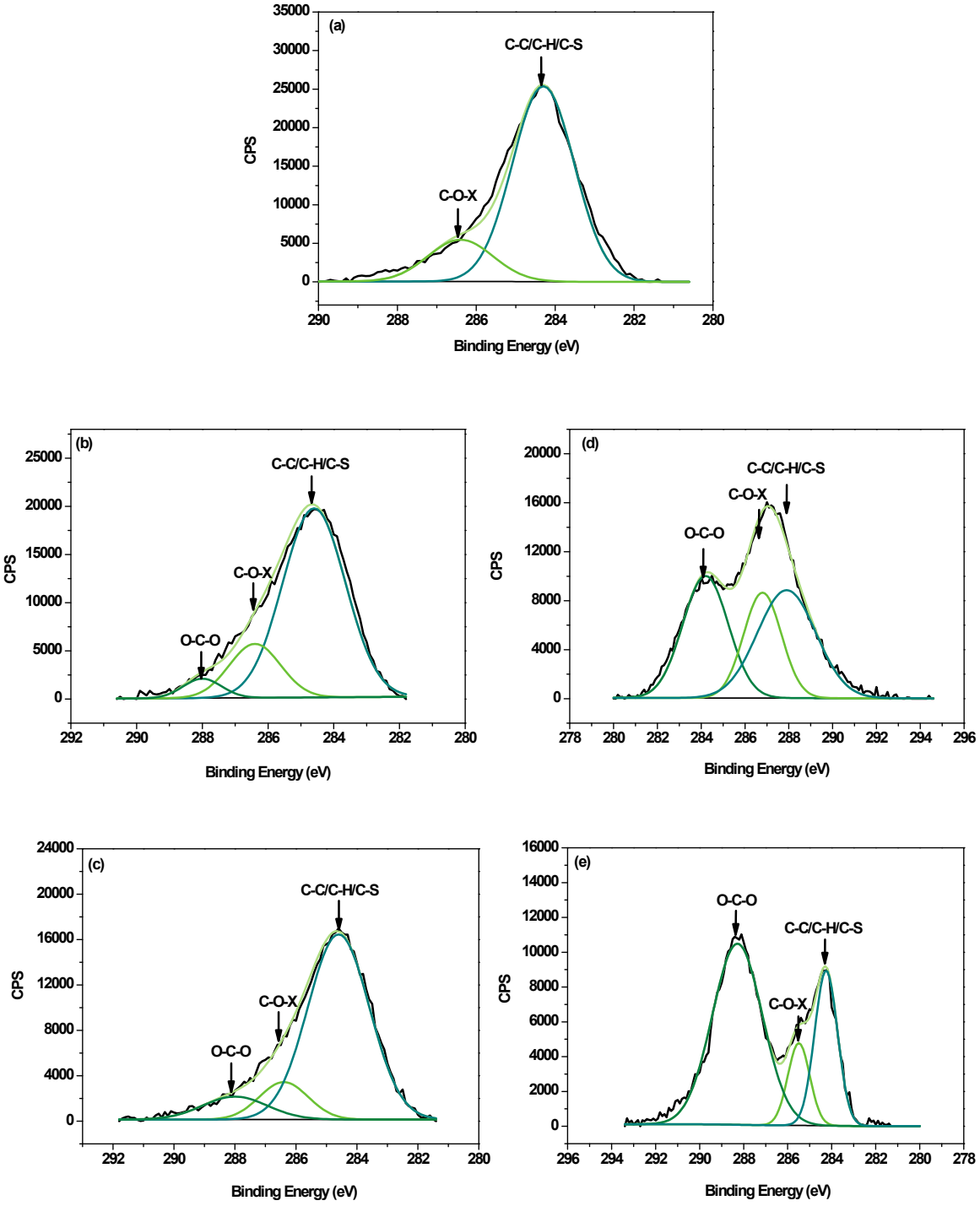

Figure S9. High-resolution XPS spectra of C1s: (a) MUD SAM surface, (b) the glucose-immobilized surface, (c) the maltose-immobilized surface, (d) the glucose-immobilized surface after enzymatic polymerization, (e) the maltose-immobilized surface after enzymatic polymerization. (Peak area (%)：(a) C-C/C-H/C-S: 81.67%, C-O-X: 18.33%; (b) C-C/C-H/C-S: 77.19%, C-O-X: 17.96%, O-C-O: 4.85%; (c) C-C/C-H/C-S: 77.51%, C-

O-X: 12.40%, O-C-O: 10.09%; (d) C-C/C-H/C-S: 35.09%, C-O-X: 25.12%, O-C-O: 39.79%; (e) C-C/C-H/C-S: 12.54%, C-O-X: 25.46%, O-C-O: 62.50%.)

Time-of-Flight Secondary Ion Mass Spectrometry (TOF-SIMS). TOF-SIMS analysis was carried out with a TRIFT II time-of-flight secondary ion mass spectrometer (Physical Electronics, USA) equipped with a $^{69}Ga^{+}$ liquid-metal primary ion source. Primary ion bombardment was done by 15 keV Ga^{+} ions with a pulsed current of 600 pA. A raster size of 100 × 100 μm was scanned and at least three different spots were analyzed. The total acquisition time was fixed to 180 s.

Fig. S10 presents the results of TOF-SIMS on the saccharide acceptors terminated SAM and the polysaccharide brushes ((a) 0 and 200 m/z, (b) 200 and 400 m/z, (c) 400 and 600 m/z, (d) 600 and 800 m/z, (e) 800 and 1000 m/z, and (f) 1000 and 1500 m/z). It shows that the saccharide-specific secondary fragment ions compose of carbon, hydrogen, and sulfur and oxygen. Additionally, the maltose acceptor terminated SAM surface is more favorable for the surface-initiated enzymatic polymerization. Because the signal of TOF-SIMS of the polysaccharide is much stronger than that introduced on the glucose acceptor terminated SAM surface.

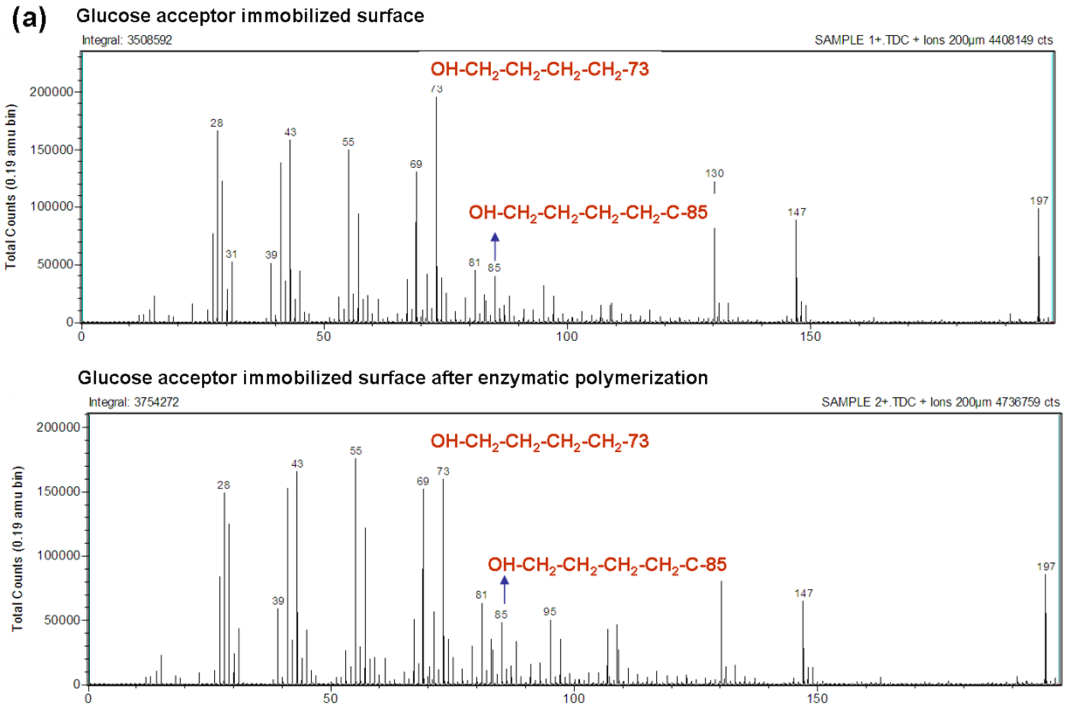

Maltose acceptor immobilized surface

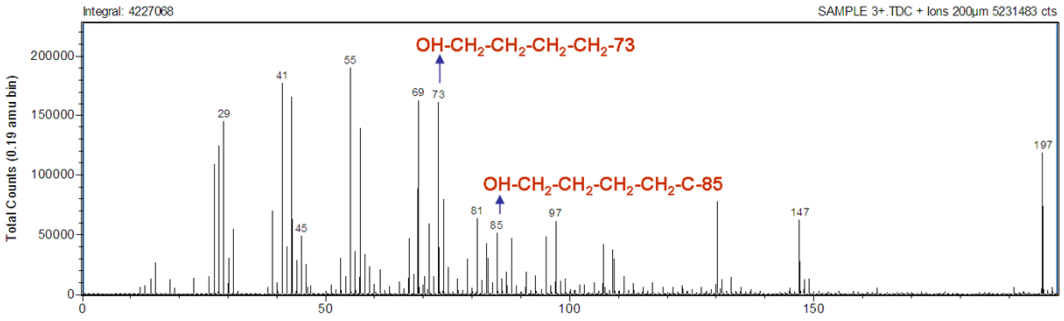

Maltose acceptor immobilized surface after enzymatic polymerization

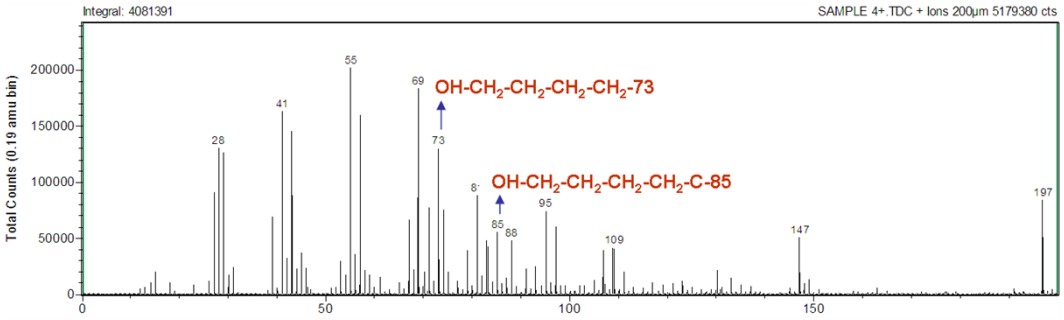

(b) Glucose acceptor immobilized surface

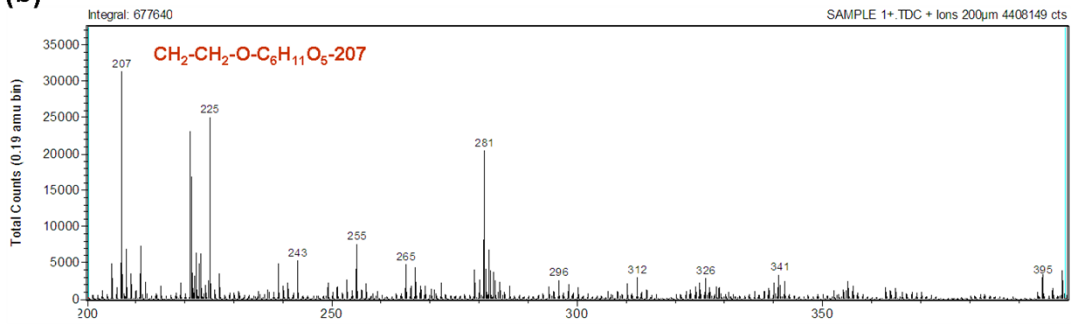

Glucose acceptor immobilized surface after enzymatic polymerization

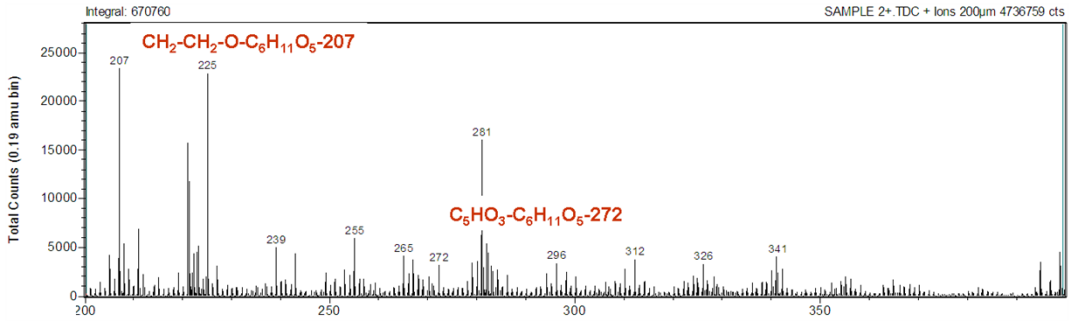

Maltose acceptor immobilized surface

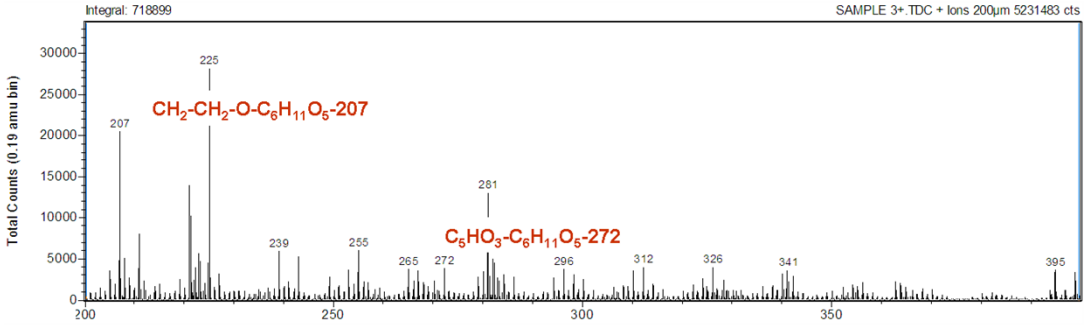

Maltose acceptor immobilized surface after enzymatic polymerization

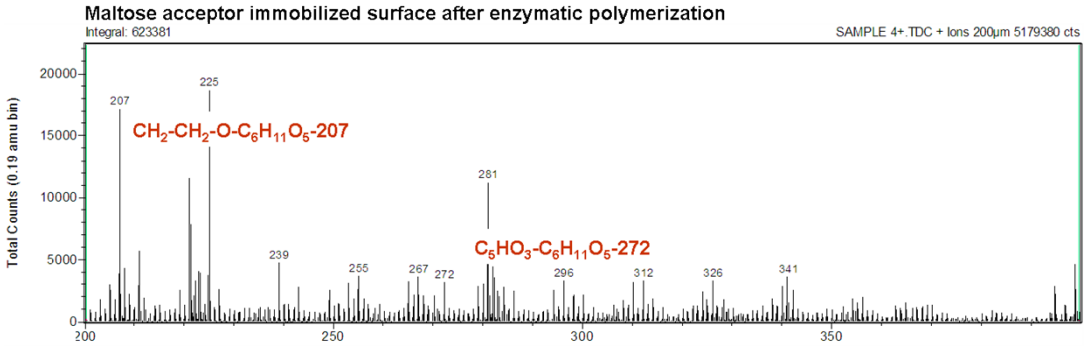

(c)

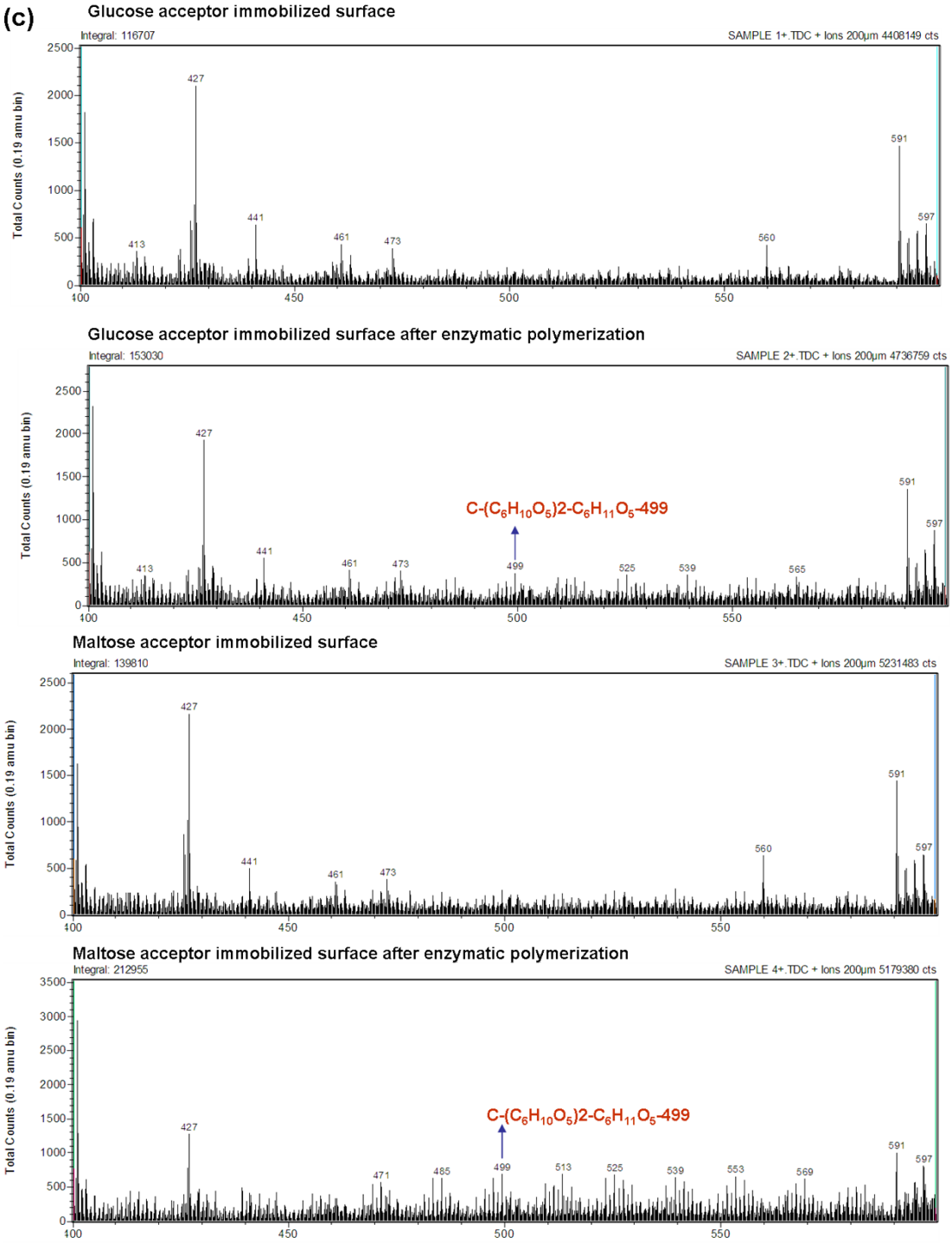
Glucose acceptor immobilized surface
Integral: 116707
SAMPLE 1+.TDC + Ions 200µm 4408149 cts
Total Counts (0.19 amu bin)
427
591
441
597
413
461
473
560
Glucose acceptor immobilized surface after enzymatic polymerization
Integral: 153030
SAMPLE 2+.TDC + Ions 200µm 4736759 cts
C-(C6H10O5)2-C6H11O5-499
499
525
539
565
Maltose acceptor immobilized surface
Integral: 139810
SAMPLE 3+.TDC + Ions 200µm 5231483 cts
Maltose acceptor immobilized surface after enzymatic polymerization
Integral: 212955
SAMPLE 4+.TDC + Ions 200µm 5179380 cts
471
485
513
553
569

(d)

Glucose acceptor immobilized surface

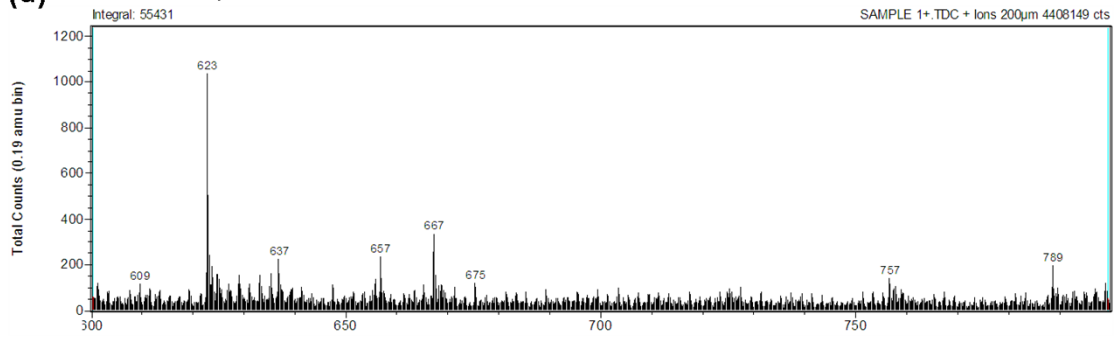

Glucose acceptor immobilized surface after enzymatic polymerization

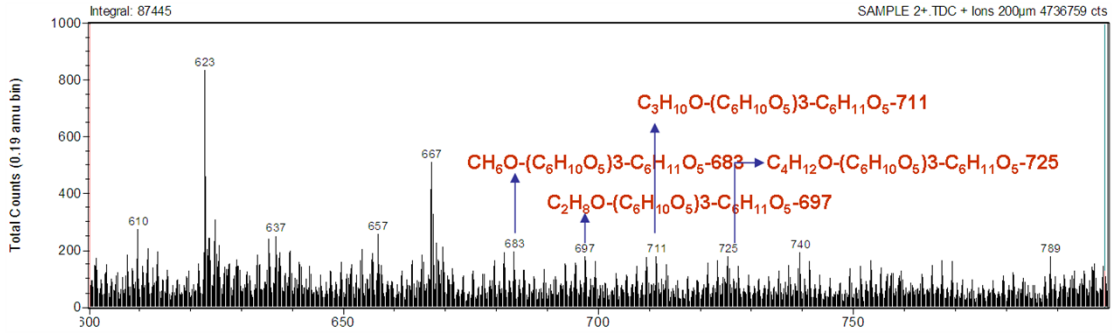

Maltose acceptor immobilized surface

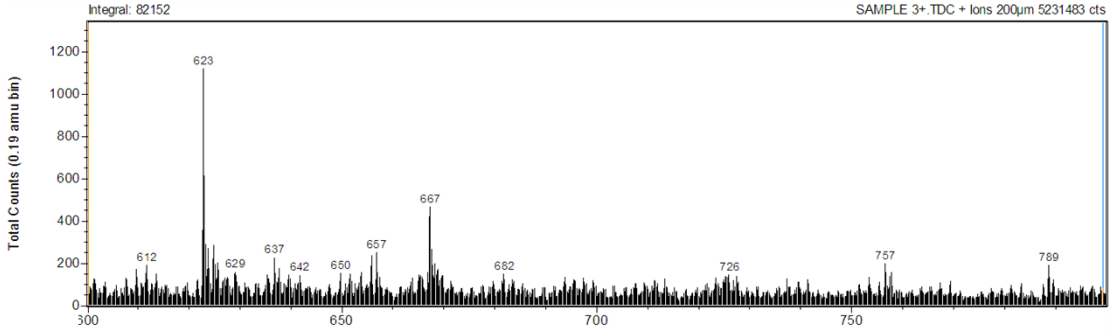

Maltose acceptor immobilized surface after enzymatic polymerization

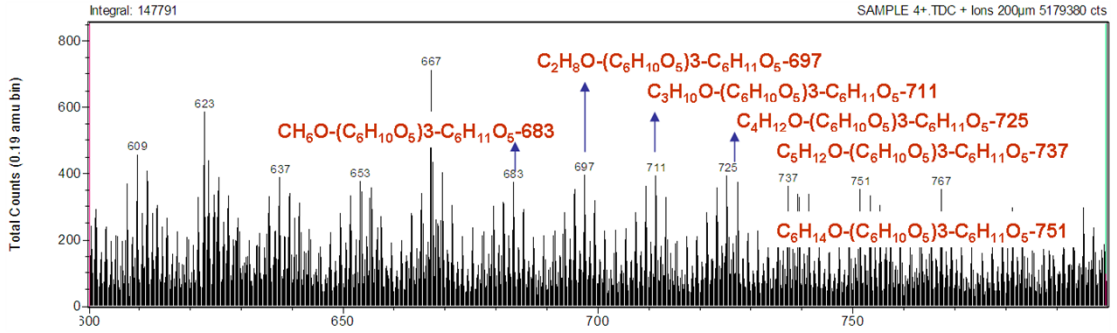

(e)

Glucose acceptor immobilized surface

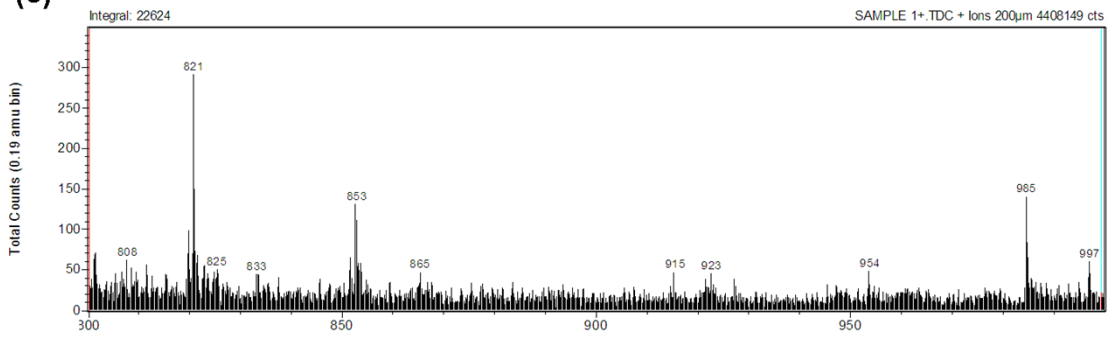

Glucose acceptor immobilized surface after enzymatic polymerization

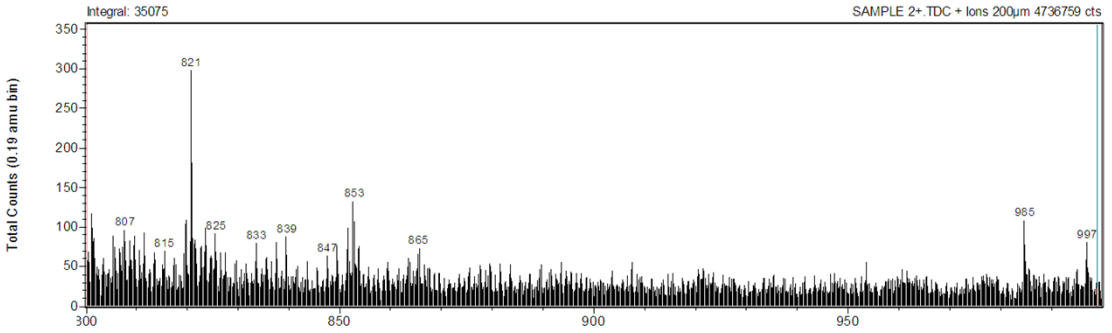

Maltose acceptor immobilized surface

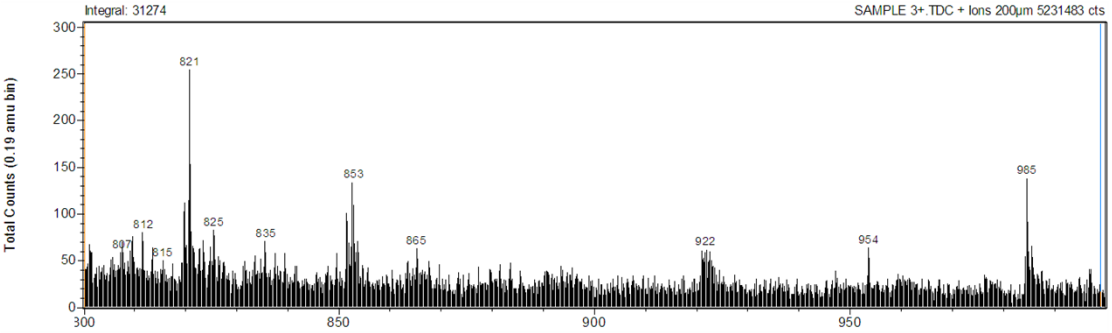

Maltose acceptor immobilized surface after enzymatic polymerization

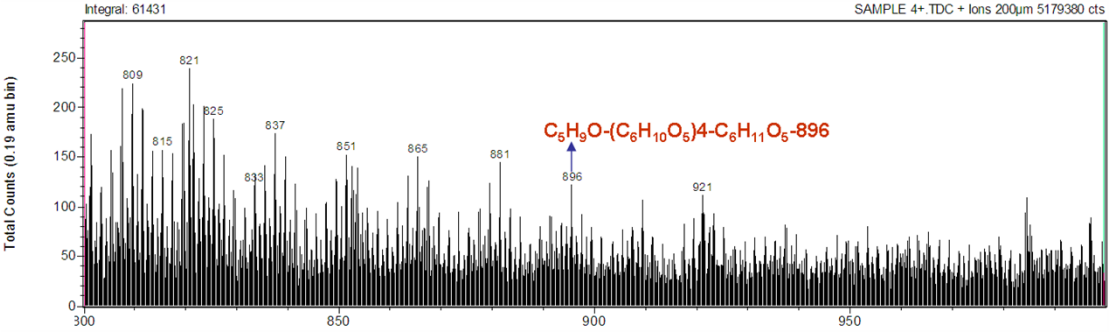

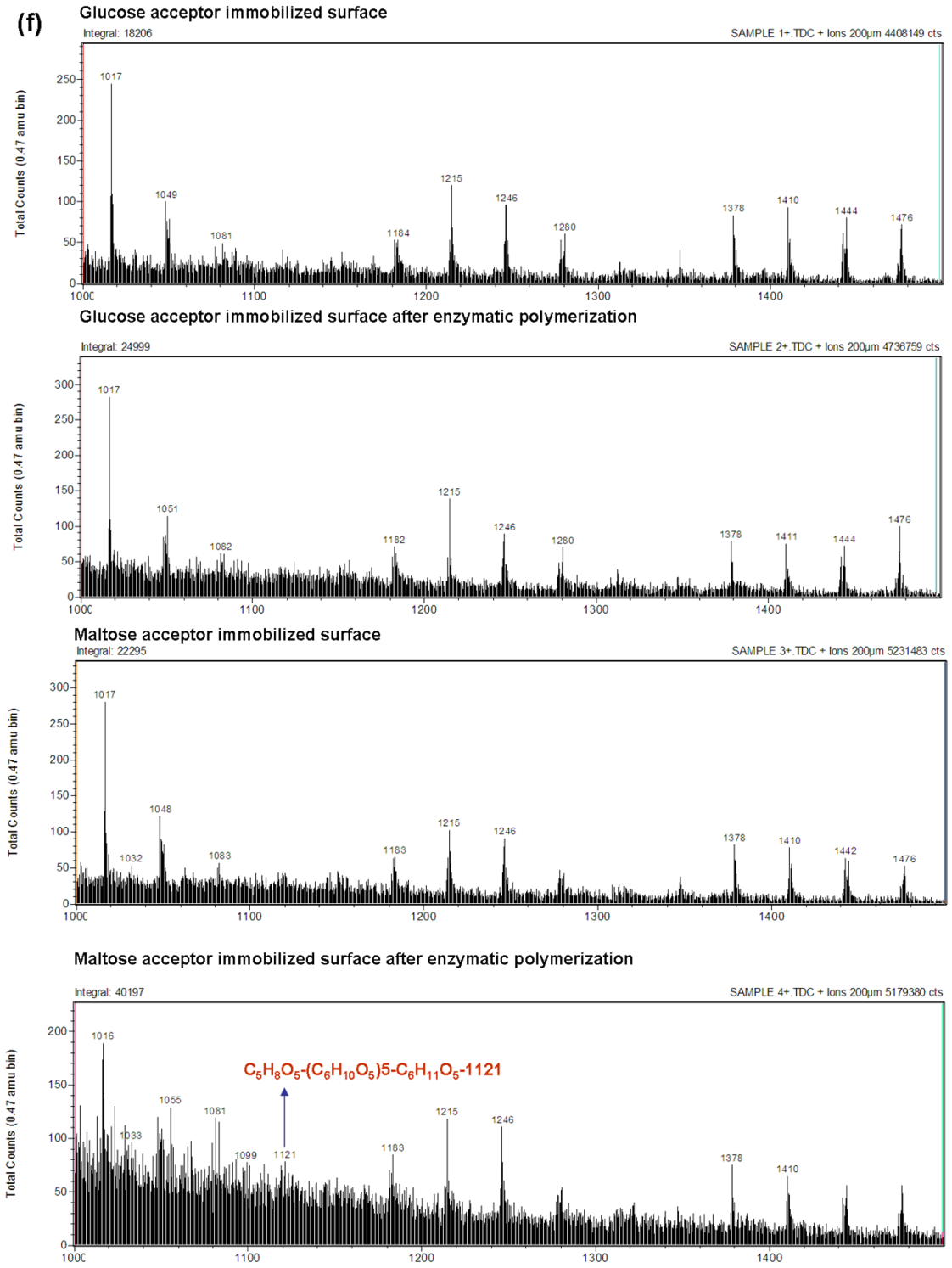

Fig. S10. Positive ToF-SIMS spectra of the glucose/maltose acceptors immobilized surface, and the glucose/maltose acceptor immobilized surface after enzymatic polymerization. The mass regions: (a) 0 and 200 m/z, (b) 200 and 400 m/z, (c) 400 and 600 m/z, (d) 600 and 800 m/z, (e) 800 and 1000 m/z, and (f) 1000 and 1500 m/z.

Atomic Force Microscopy (AFM). AFM images of the saccharide acceptors immobilized surfaces before and after enzymatic polymerization were obtained using a TM Lumina atomic force microscope (Nano IV, Veeco, USA), operated in tapping mode. Oxide sharpened SiN_3 cantilevers were used with a quoted spring constant of 0.04 N m^{-1}. Data were captured at a rate of 10 m s^{-1} in the z direction and a scan rate of 4 Hz. Fig. S11 shows the AFM images of the whole modified QCM chip surfaces and Fig. S12 shows the thickness of these surfaces measured by the peak-to-trough height of AFM. It was found that the blank MUD SAM surface has a peak-to-trough height of 1.22 ± 0.2 nm, while this value changes slightly to 1.62 ± 0.2 nm and 2.09 ± 0.2 nm for the glucose and the maltose immobilized surfaces, respectively. Furthermore, the thickness changes to 1.76 ± 0.2 nm and 2.63 ± 0.2 nm after enzymatic polymerization. The thickness change is in good agreement with that measured by ellipsometry. In addition, it indicates there are no bound enzymes on the newly prepared polysaccharide brushes because the diameter of DSase molecule is 6.0 nm. All these data suggest that the enzymatic polymerization has been carried out successfully on the small saccharides acceptors immobilized surfaces and the enzymatic activity is higher on the maltose acceptor immobilized surface.

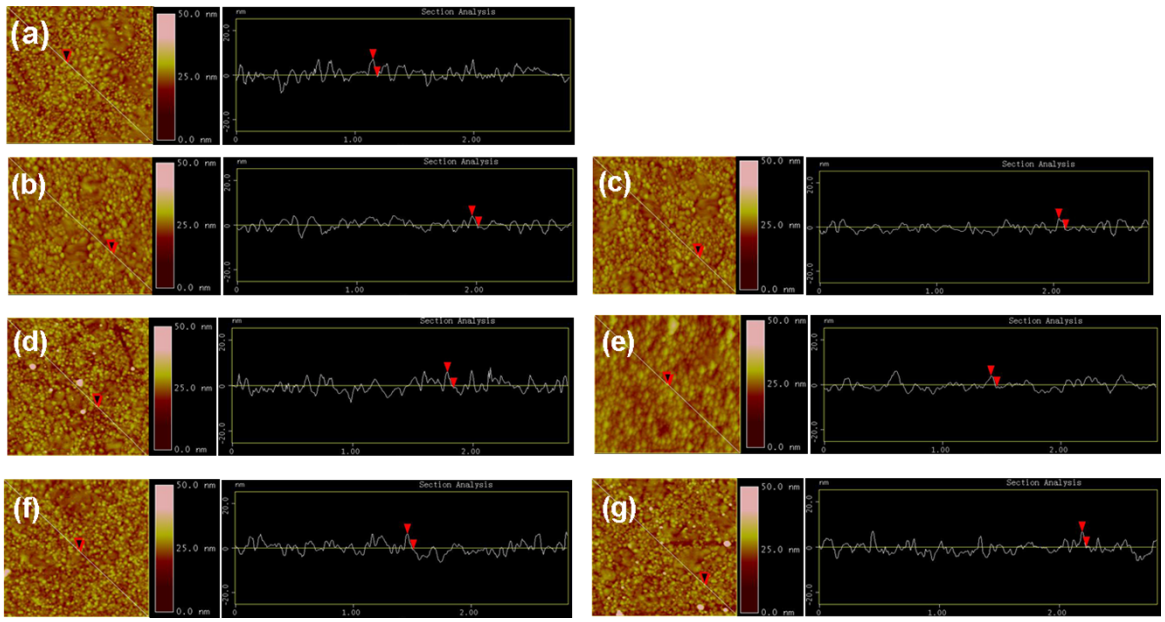

Fig. S11. AFM images of (a) the MUD SAM surface, (b) the GPA immobilized surface, (c) the MOA immobilized surface, (d) the glucose acceptor immobilized surface, (e) the maltose acceptor immobilized surface, (f) the glucose acceptor immobilized surface after enzymatic polymerization, (g) the glucose acceptor immobilized surface after enzymatic polymerization.

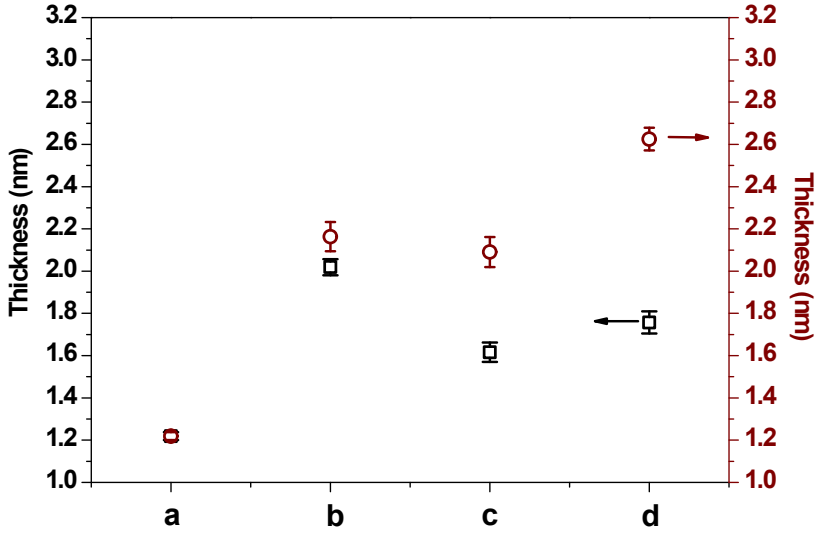

Fig. S12. Thickness of the layers measured by AFM: a. MUD immobilized surfaces (SAM); b. the GPA (□) and MOA (○) immobilized surfaces; c. the glucose (□) and maltose (○) immobilized surface; d. the glucose (□) and maltose (○) immobilized surface after enzymatic polymerization.

Specific adsorption of proteins to the polysaccharide brushes. As a control surface, the saccharide acceptor immobilized surfaces were also measured for comparison. Fig. S13~S16 show the typical QCM curves for protein adsorption. A stable baseline signal was established by flowing PBS buffer (0.1 M, containing 0.1 mM $CaCl_2$, 0.1 M NaCl and 0.1 mM $MnCl_2$ for Con A, and pH 7.4) at a rate of 25 μL/min through the sensor. Different protein solutions (10 μg/mL) of BSA, RCA_{120}, and Con A were injected into the channel, respectively. After adsorption for a fixed time at 25 °C, PBS buffer was used to remove unbound or loosely bound proteins from the sensor surface. The adsorbed amounts of proteins can be calculated from the QCM curves. On the one hand, it was found that more amounts of Con A are adsorbed on not only the saccharide acceptors immobilized surfaces but the newly prepared polysaccharide brushes due to the specific interaction between Con A and the glucosyl/maltosyl-residues. On the other hand, both these ultra-hydrophilic glycosylated surfaces show highly non-specific adsorption to BSA and RCA_{120}. Furthermore, compared with the saccharide acceptors immobilized surfaces, the newly prepared polysaccharide brushes adsorb more Con A molecules due to the more nonreducing glucosyl-residues of the polysaccharide brushes.

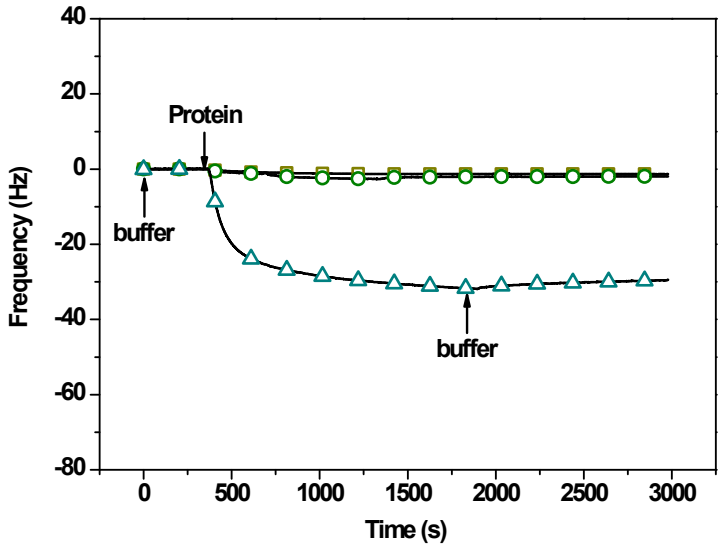

Fig. S13. QCM curves for protein adsorption on the glucose acceptor immobilized surface. (□: BSA, ○:RCA_{120}, Δ:Con A)

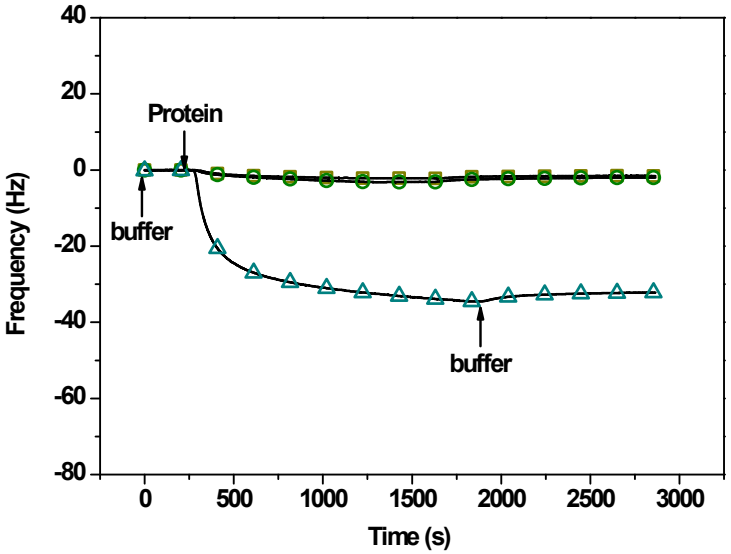

Fig. S14. QCM curves for protein adsorption on the maltose acceptor immobilized surface. (□: BSA, ○:RCA_{120}, Δ: Con A)

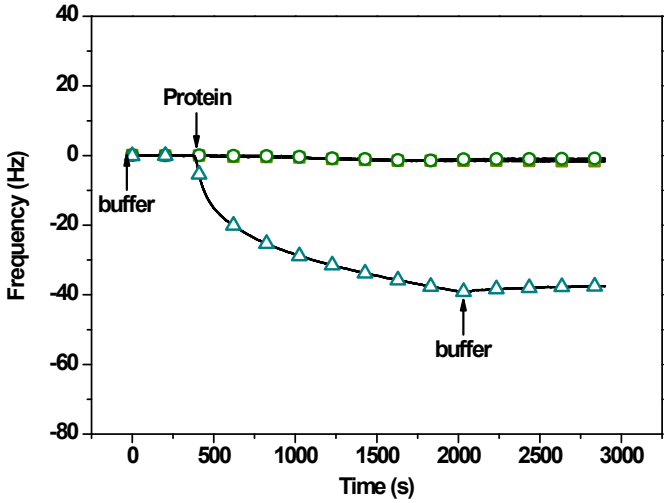

Fig. S15. QCM curves for protein adsorption on the glucose acceptor immobilized surface after enzymatic polymerization. (□: BSA, ○: RCA_{120}, Δ: Con A)

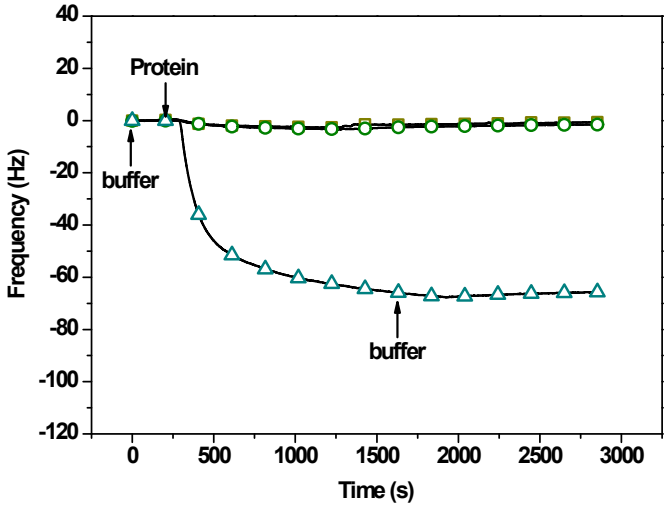

Fig. S16. QCM curves for protein adsorption on the maltose acceptor immobilized surface after enzymatic polymerization. (□: BSA, ○: RCA_{120}, Δ: Con A)

Fluorescence Microscopic Observation. The specific adsorption of FITC-protein on the polysaccharide brushes was also confirmed by fluorescence microscopy. The samples were immersed in a PBS solution of FITC-BSA, FITC-RCA_{120}, FITC-Con A (20.0 μg/mL) for a prescribed time at room temperature, respectively. They were then washed softly by immersing in PBS, and this procedure was repeated three times with fresh PBS. After that, the chips were dried under vacuum at room temperature. Fluorescence images were taken on an optical microscope (Eclipse TE2000, Nikon, Tokyo, Japan) equipped with a highly sensitive CCD camera (ORCA-ER, Hamamatsu Photonics, Shizuoka, Japan). The observation was made on at least three spots for each sample. Fig. S17 shows

the typical fluorescence images of FITC-protein absorbed on the MUD SAM surface, the glucose/maltose acceptor immobilized surfaces, and the glucose/maltose acceptor immobilized surfaces after enzymatic polymerization. It was found that FITC-Con A can be specifically adsorbed on not only the saccharide acceptors immobilized surfaces but the saccharide acceptors immobilized surfaces after enzymatic polymerization. And the adsorbed amount of FITC-Con A increases after enzymatic polymerization. It seems that the maltose acceptor immobilized surface after enzymatic polymerization has the most adsorption amount of FITC-Con A. Besides, all the glycosylated surfaces show highly non-specific adsorption to FITC-BSA and FITC-RCA_{120}. All these results suggest that the DSase-catalyzed surface-initiated enzymatic polymerization has been carried out successfully and the maltose acceptor immobilized surface is more favorable for this enzymatic reaction. Fig. S18 presents the effect of sucrose concentrations on the enzymatic polymerization. The fluorescence images of FITC-Con A absorbed on the polysaccharide brushes show that there are more glucosyl moiety can be polymerized to the surfaces upon increasing the sucrose concentrations.

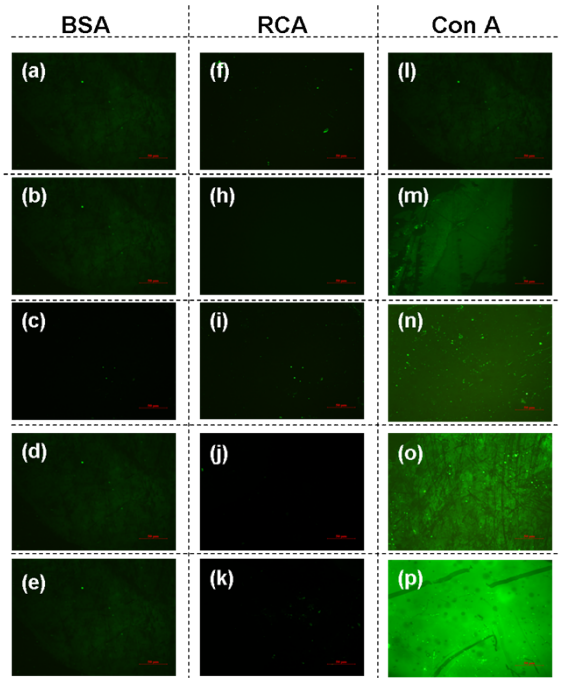

Fig. S17. Fluorescence images of FITC-protein absorbed on (a), (f), (l) the MUD SAM surface; (b), (h), (m) the glucose acceptor immobilized surface; (c), (i), (n) the maltose acceptor immobilized surface; (d), (j), (o) the glucose acceptor immobilized surface after enzymatic polymerization; (e), (k), (p) the maltose acceptor immobilized surface after enzymatic polymerization.

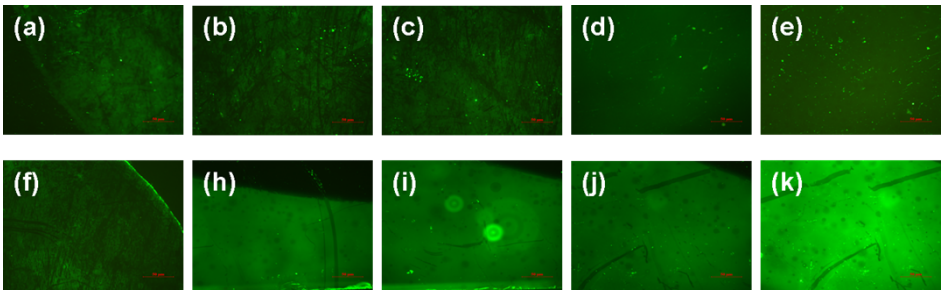

Fig. S18. Fluorescence images of FITC-Con A absorbed on: (a~e) the glucose and (f~k) the maltose acceptors immobilized surface after enzymatic polymerization. (Effect of different sucrose concentrations on the enzymatic polymerization: (a) (f) 2.5 mM; (b) (h) 5 mM; (c) (i) 10 mM; (d) (j) 15 mM; (e) (K) 15 mM.)

Reference

[1] V. S. R. Rao, N. Yathindr, P. Sundarar, *Biopolymer* **1969**, 8, 325–333.

[2] S. Immel, F. W. Lichtenthaler, *Starch/Stärke* **2000**, 1, 1–8.

[3] P. M. Dietrich, T. Horlacher, P. L. Girard-Lauriault, T. Gross, A. Lippitz, H. Min, T. Wirth, R. Castelli, P. H. Seeberger, W. E. S. Unger, *Langmuir* **2011**, 27, 4808–4815.